Axion dark matter detection by laser spectroscopy of ultracold molecular oxygen: a proposal

2015 New J. Phys. 17 113025

(http://iopscience.iop.org/1367-2630/17/11/113025)

New Journal of Physics
The open access journal at the forefront of physics

Deutsche Physikalische Gesellschaft DPG
IOP Institute of Physics

Published in partnership with: Deutsche Physikalische Gesellschaft and the Institute of Physics

OPEN ACCESS

RECEIVED
28 May 2015

REVISED
9 September 2015

ACCEPTED FOR PUBLICATION
20 October 2015

PUBLISHED
9 November 2015

PAPER

Axion dark matter detection by laser spectroscopy of ultracold molecular oxygen: a proposal

L Santamaria[1], **C Braggio**[2], **G Carugno**[2], **V Di Sarno**[1], **P Maddaloni**[1,3] **and G Ruoso**[4]

[1] CNR-INO, Istituto Nazionale di Ottica, Via Campi Flegrei 34, I-80078 Pozzuoli, Italy
[2] Dipartimento di Fisica "G. Galilei", Università di Padova, Via F. Marzolo 8, I-35131 Padova, Italy
[3] INFN, Istituto Nazionale di Fisica Nucleare, Sez. di Firenze, Via G. Sansone 1, I-50019 Sesto Fiorentino, Italy
[4] INFN, Laboratori Nazionali di Legnaro, Viale dell'Università 2, I-35020 Legnaro, Italy

E-mail: pasquale.maddaloni@ino.it

Keywords: axion dark matter, buffer gas cooling, laser spectroscopy

Abstract

Generalizing Sikivie's approach (Sikivie 2014 *Phys. Rev. Lett.* **113** 201301), according to which dark matter axions may induce transitions between Zeeman states in an atomic system, an experiment based on a molecular gas is proposed for a search in the axion mass range between 1.4 and 1.9 meV. In particular, a $^{16}O_2$ sample is brought to the temperature of 280 mK via buffer-gas cooling and then subjected to an external magnetic field; axion-driven transitions are eventually detected by resonance-enhanced multi-photon ionization spectroscopy.

1. Introduction

An outstanding problem in contemporary physics is that of dark matter (DM) whose existence is generally accepted on the basis of strong astrophysical evidence, but the composition of which is still unclear [2, 3]. The most authoritative candidates for DM are weakly interacting massive particles and axions [4]. The latter have been introduced to provide a solution to the strong CP problem [5–8] and, in view of their weak interaction with ordinary matter, have become an aspirant for the DM component of galactic halos. Several detection schemes have been proposed to detect DM axions [9], some of which are already being implemented. The conversion of axions into photons in a microwave cavity permeated by an external magnetic field, originally proposed by Sikivie [10, 11], has been pursued by several groups [12–14]. Other proposed schemes include: the conversion of axions into magnons in a ferromagnet [15, 16]; the study of the nuclear precession of a material which can be modified by its interaction with the axion [17, 18]; the presence of energy shifts or nonzero nucleon electric dipole moments arising in atomic systems from the coupling of axions to gluons [19]; the excitation of a high n transition in a Rydberg atom [20]. Lately, it has also been suggested that DM axions may induce magnetic dipole (M1) transitions between atomic or molecular states that differ in energy by an amount equal to the axion mass [1].

Based on this idea, here we detail the proposal of an experiment which aims at detecting molecular transitions in a gas system where axions in the 10^{-3} eV mass range are absorbed. For this purpose, first we have to identify a molecular system with two magnetic sublevels whose energy difference can be tuned via the Zeeman effect to the desired axion mass value. These two levels, let us say a and b, will respectively represent the lower and upper level of what we will hereafter call the axion transition. Then, by cooling the gas sample such that there are no molecules in b, as a result of the exposition to the DM axion field, $a \rightarrow b$ transitions will be induced with a unit-time rate, $\mathcal{R}_{ab}$, of few events per mole of molecules (provided that M1 selection rules are satisfied) [1]. Finally, an appropriate detection technique must be used to reveal with almost 100% efficiency the presence of the molecules promoted into level b. From an experimental point of view, this involves the preparation of a sub-Kelvin, mole-sized molecular gas sample through a buffer-gas-cooling (BGC) process in a ^{3}He environment. In addition, the molecular species should be sensitive enough to the application of an external magnetic field and well-suited to a single-particle spectroscopic interrogation technique as well. In this respect, the oxygen molecule, $^{16}O_2$, offers three major advantages. First, it is undoubtedly one of the best investigated molecules on

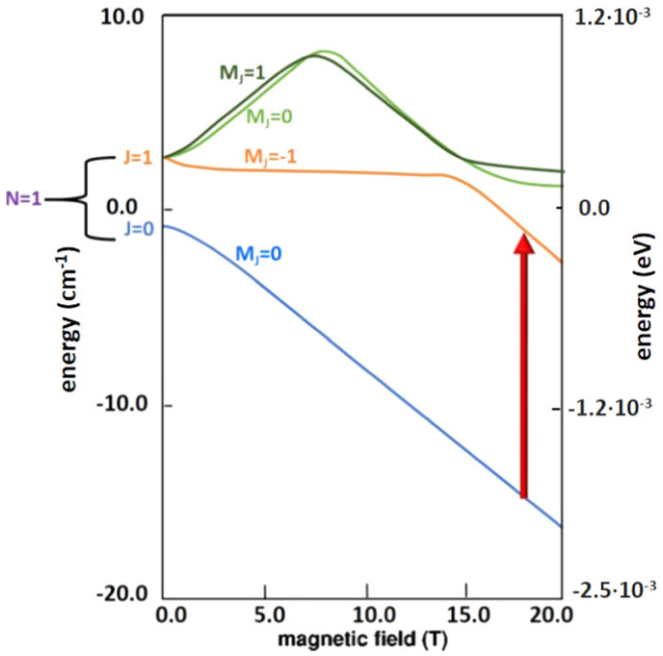

Figure 1. Illustration of the Zeeman effect for the $N = 1$ rotational levels in the $X^3\Sigma_g^-(v = 0)$ ground state of $^{16}O_2$ (the $J = 2$ component is omitted for a clear view). The axion transition is indicated by the red arrow.

Earth, in terms of spectroscopy as well [21]. In particular, it has already been used for spectroscopic tests of fundamental physics, such as the symmetrization postulate on spin-0 nuclei [22, 23], and as well employed in a number of high-sensitivity laser-based detection schemes including magnetic rotation spectroscopy [24], polarization-dependent cavity ring-down spectroscopy [25], and resonance-enhanced multi-photon ionization (REMPI) spectroscopy [26]. Second, $^{16}O_2$ is a prototypical paramagnetic molecule with a high magnetic moment ($2\mu_B$). Third, it has already been cooled down to few Kelvin in BGC experiments [27].

The paper is organized as follows. In section 2, we focus on the choice of the $^{16}O_2$ transition that is most eligible for the axion detection; crucial issues of the gas sample preparation in a BGC machine are also addressed from a theoretical viewpoint. Then, section 3 deals with the REMPI spectroscopic detection of the axion-induced absorption events. Following this discussion, section 4 gives the details of the experimental apparatus. Finally, in section 5, we conclude.

2. Sample preparation

Let us start by considering the $X^3\Sigma_g^-(v = 0)$ ground state of $^{16}O_2$. Only rotational levels of odd rotational angular-momentum quantum number N are populated in $^{16}O_2$ because of restrictions imposed by the $I = 0$ bosonic nature of the oxygen nuclei. Each rotational level is split into three spinrotational components that are additionally labeled by the total angular-momentum quantum number J (J can take the values $N - 1$, N and $N + 1$ and the corresponding levels are often referred to as the F_3, F_2 and F_1 component of the p-type triplet, respectively). Upon application of an external magnetic field, $\boldsymbol{B}$, each spinrotational component is further split into $2J + 1$ magnetic sublevels; these are labeled by the magnetic quantum number M_J ($M_J = -J, -J + 1, ..., J$), namely the projection of J onto the direction of $\boldsymbol{B}$. In this coupling scheme, selection rules for M1 transitions require: $\Delta J = 0, \pm 1$ ($J = 0 \not\leftrightarrow 0$), $\Delta M_J = 0, \pm 1$, and $\pi_b = \pi_a$, where π_a (π_b) denotes the parity of the transition's lower (upper) level. Next, we adopt the notation $W(r, B)$ to represent the energy of the $r \equiv (N, J, M_J)$ magnetic sublevel as a function of B. The energy-level diagram displayed in figure 1 illustrates the Zeeman effect in the $X^3\Sigma_g^-(v = 0)$ state up to a magnetic field intensity of $B = 20$ T by [25].

At this point in the discussion, we choose the rotational level $(N = 1, J = 0, M_J = 0) \equiv a$ and $(N = 1, J = 1, M_J = -1) \equiv b$ as the lower and upper level of the axion transition, respectively. This determines the maximum axion mass range that can be explored according to the following reasoning. In order to realize a mole-sized population of $^{16}O_2$ molecules in level a, while keeping level b depopulated, the energy difference $W_{ba}(B) \equiv W(b, B) - W(a, B)$ must satisfy the condition $Q(B, T) \equiv N_A \exp[-W_{ba}(B)/(k_B T)] < 0.1$ with k_B being the Boltzmann constant, N_A the Avogadro number, and T the gas temperature [1]. Now, as explained later, the minimum T value which provides a helium-3 vapour pressure that is capable to effectively cool N_A oxygen

molecules is $T_{He} \simeq 277$ mK; as a result, $B_{min} = 12$ T is found, corresponding to $W_{ba}(B_{min}) = 11\ cm^{-1}$ (1.4 meV) with $Q(B_{min}, T_{He}) = 0.09$. Concerning the upper end of the axion mass interval, it is worth remarking that, besides technical difficulties, the Zeeman splitting $W_{ba}(B)$ tends to saturate for magnetic fields above $B_{max} = 18$ T; this amounts to $W_{ba}(B_{max}) = 15.5\ cm^{-1}$ (1.9 meV) with $Q(B_{max}, T_{He}) = 1.5 \times 10^{-10}$.

The above argument presupposes, however, complete rotational thermalization of the molecular sample within the BGC source under reasonable experimental conditions. To ascertain this point, we have to get a little more into the details of the BGC process. Here, both translational and internal degrees of freedom of the desired molecular species, at initial temperature T_0, are cooled in a cryogenic cell via collisions with a thermal bath of helium-3 (buffer gas) at temperature T_{He} and density n_{He}. After a characteristic number of collisions N_{coll}, the molecular temperature becomes arbitrarily close to equilibrium with the buffer gas, $T(N_{coll}) = T_{He} + (T_0 - T_{He})\exp(-N_{coll}/\chi)$, where $\chi = (m + m_{He})^2/(2\ m \cdot m_{He})$ (m and m_{He} denote the molecular and the helium-3 mass, respectively). With this in mind, let us now calculate the minimum $^{16}O_2$-in-^{3}He collisional path-length (random walk) which is needed to thermalize N_A molecules. Since the order of magnitude for He-molecule elastic-collision (rotational-relaxation) cross sections is $10^{-18}\ m^{-2}$ ($10^{-20}\ m^{-2}$) [28–30], around 100 collisions are required to relax a rotational state. Denoting with $P(E_i)$ the probability that the ith oxygen molecule has not reached thermalization after traveling the distance L in the buffer gas (E_i is the corresponding event), the probability $\mathcal{P}_{N_A}$ that even one molecule (in N_A molecules) evades the thermalization process is given by $\mathcal{P}_{N_A} \equiv P(\cup_{i=1}^{N_A} E_i)$. According to Boole's inequality, this probability is smaller than the sum of the probabilities of the separated events, $\mathcal{P}_{N_A} < \sum_{i=1}^{N_A} P(E_i) \equiv P_s$. This latter quantity is given by

$$P_s = N_A \frac{\sum_{i=1}^{\infty} B(\nu_i) P(E_i)}{\sum_{i=1}^{\infty} B(\nu_i)} \simeq N_A \frac{\sum_{i=1}^{M} B(\nu_i) P(E_i)}{\sum_{i=1}^{M} B(\nu_i)}, \tag{1}$$

where M is a number high enough and the $P(E_i)$'s are weighted by the Maxwell–Boltzmann distribution of molecular velocities:

$$B(\nu_i) = 4\pi \sqrt{\frac{m}{2\pi k_B T}}\ \nu^2 \exp\left[-m\nu^2 / (2k_B T)\right]. \tag{2}$$

Equation (1) is then computed by a direct Monte Carlo simulation for $T_{He} = 280$ mK and the corresponding vapor density, $n_{He} = 3 \times 10^{16}\ cm^{-3}$[31]; for $L = 1$ cm, a value close to 10^{-6} is already found for P_s. Then, if $P_s \ll 1$, *a fortiori* this will be true for $\mathcal{P}_{N_A}$. This means that, under the aforementioned experimental conditions, all the oxygen molecules contained in the buffer gas cell will be in level a.

The possibility of spurious collision excitation events caused by the background gas is also considered. To this aim, the kinetic energy term $(1/2) m_{He} v_{He}^2$ is equated to $W_{ba}(B_{min}) = 11\ cm^{-1}$; this yields the minimum velocity value needed to promote an oxygen molecule to the axion transitions upper level, $\tilde{v}_{He} = 295\ m\ s^{-1}$. Finally, the integral of the Maxwell–Boltzmann distribution is computed from $\tilde{v}_{He}$ to ∞ and multiplied by N_A to provide the number of He-3 atoms exceeding this velocity. The result, which represents an overestimation of the number of spurious collision excitation events, is well below the unity. Furthermore, blackbody radiation effects are quantitatively addressed. For this purpose, the power emitted by the total internal surface area of the experimental setup, $\mathcal{A}$, is first calculated by the Stefan–Boltzmann law as $P_{em}^{tot} = \mathcal{A}\sigma T_S^4$. Then, defining $\nu_0 \equiv W_{ba}(B_{min})$ and denoting with $\Delta\nu$ the Doppler width of molecular oxygen (calculated at ν_0 and for $T = T_S$), the number of blackbody photons (per unit time) in the frequency interval $[\nu_0 - \Delta\nu, \nu_0 + \Delta\nu]$ is derived as

$$N_{bb}(\nu_0 - \Delta\nu \leqslant \nu \leqslant \nu_0 + \Delta\nu) = \frac{P_{em}^{tot}}{h\nu_0} \frac{\int_{\nu_0 - \Delta\nu}^{\nu_0 + \Delta\nu} \nu^3 \left[e^{\frac{h\nu}{k_B T}} - 1\right]^{-1} d\nu}{\int_0^{\infty} \nu^3 \left[e^{\frac{h\nu}{k_B T}} - 1\right]^{-1} d\nu}. \tag{3}$$

For $T_S \simeq 0.5$ K, $N_{bb} \simeq 6 \times 10^{-3}\ s^{-1}$ is found; since only a very small fraction of N_{bb} is absorbed by the molecular oxygen due to the low strength of the axion transition, this implies a negligible blackbody-radiation induced transition rate. In conclusion, it is worth pointing out that, from an experimental point of view, an effective way to discriminate against any spurious effect is to exploit the directional character of the interaction between axions and ordinary matter by counter-checking the signal at a second angle (at 90° with respect to the first one) with a rotatable apparatus.

3. REMPI spectroscopic detection

The next step is to detect the molecules promoted by the DM axion field into level b. Since very few events are expected, an extremely sensitive spectroscopic technique must be implemented, which is particularly able to

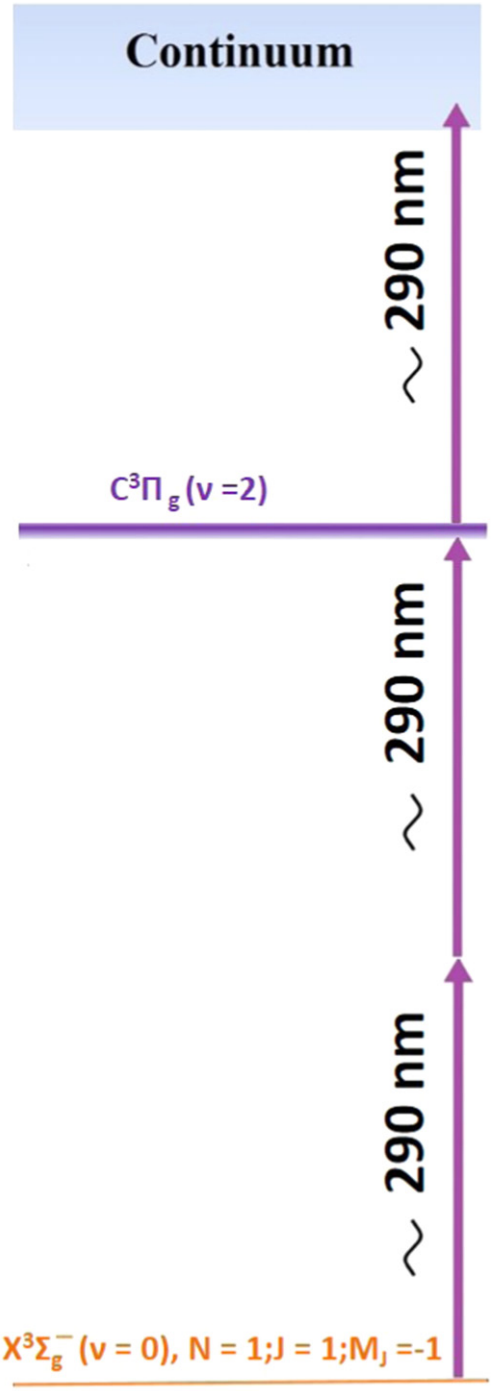

Figure 2. Energy-level diagram involved in the (2+1)REMPI spectroscopic detection. The oxygen molecules promoted by the axion field into the ($N = 1, J = 1, M_J = -1$) level are subsequently ionized by using laser pulses tunable around 287 nm (violet arrows).

detect an axion absorption occurrence before collisions with surrounding particles may cause decay from level *b*. As already mentioned, molecular oxygen is well-suited to the (2+1)REMPI interrogation scheme. In general, this method involves a resonant single or multiple photon absorption to an electronically excited intermediate state followed by another photon which ionizes the molecule; the ionization product is then detected with almost 100% efficiency usually by a micro-channel plate (MCP). Specifically, the (2+1) symbol means that two photons must be absorbed to excite the molecule in the intermediate state and one photon to ionize the molecule. With reference to figure 2, in the $^{16}O_2$ case, (2+1)REMPI spectroscopy can be carried out exploiting the $C^3\Pi_g(\upsilon = 2)$ component as the intermediate state by using laser pulses tunable around 287 nm [32, 33]. Anomalously, the rotational levels belonging to this component are characterized by far long lifetimes (in other words, they are much less predissociative than usual), thus favorably exhibiting enough narrow line widths ($<$ 6 cm^{-1}) [34]. Therefore, calling w_{laser} the laser linewidth and w_{rot}^{int} the width of the narrowest rotational level in

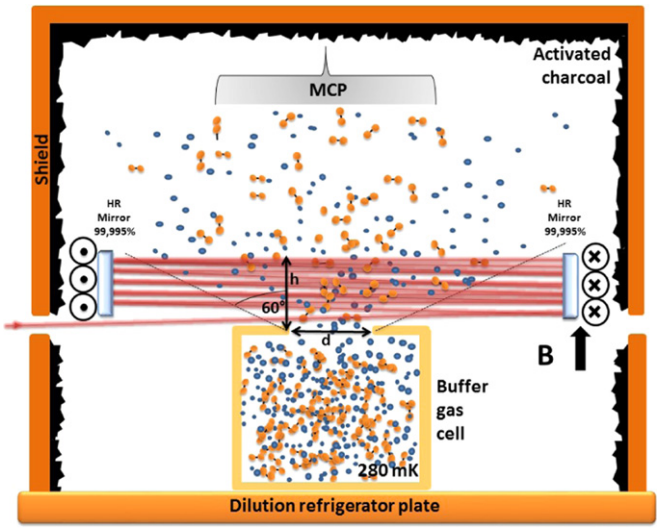

Figure 3. Schematic layout of the experimental apparatus. The 280 mK $^{16}O_2$ beam emerging from the BGC source is subjected to REMPI spectroscopy. Any ionization product, only possible as a consequence of axion-driven $a \rightarrow b$ absorption events, is eventually detected by a micro-channel plate. The actual signal depends on the specific molecular transition used, the molecule's polarization direction (determined by the magnetic field), and the momentum distribution of the axions (varying with time of day and of year) [1].

the $C^3\Pi_g(v = 2)$ component, the condition $W_{ba}^{\min} = W_{ba}(B = 12\ \mathrm{T}) = 11\ \mathrm{cm}^{-1} > \max(w_{\mathrm{laser}}, w_{\mathrm{rot}}^{\mathrm{int}})$ can be easily satisfied. This means that a and b levels of the axion transition are fully resolved by (2+1)REMPI spectroscopy.

4. Experimental apparatus and results

A schematic representation of the experimental apparatus is shown in figure 3. Machined from Cryo-G10, the BGC cell is thermally anchored to the mixing chamber of a dilution refrigerator by high-purity copper braids [35]. Thermal conductivity along the cell length is provided by copper wires running vertically along the outer Cryo-G10 walls. A hole with a diameter of $d = 15$ cm is made in one of the walls to let the $^{16}O_2$ molecules escape from the cell into a second chamber whose internal surface is covered by a layer of activated charcoal. At cryogenic temperatures, this acts as a pump with a speed of a few thousands $\mathrm{dm}^3\ \mathrm{s}^{-1}$, creating a high-vacuum region. The (2+1)REMPI interrogation then takes place in the bore of 57 cm diameter superconducting magnet (coaxial to the BGC cell) which creates a homogeneous magnetic field of up to 18 T along a traveling distance $h = 12$ cm. Two facing high-reflectivity ($R_m = 99.995\%$) mirrors are used to accomplish multiple reflections of the laser beam so as to draw a pattern of a large number of spots, N_{refl}, through the trapezoidal section of the (truncated-cone-shaped) molecular beam. In this way, the laser radiation interacts with a fraction $\mathcal{F} = (N_{\mathrm{refl}}\pi\ w^2)/(h\ d + h^2\ \tan\theta)$ of the molecular flux, where w denotes the laser beam waist and $\theta = 60°$ is the molecular beam divergence. Then, for $w = 1$ mm and $N_{\mathrm{refl}} = 13\ 500$, $\mathcal{F} \simeq 1$ is found. At the end of the magnet, a micro-channel plate is then employed to collect the (2+1)REMPI ionization products. Capillary filling is used to inject both the molecular oxygen and the He-3 buffer gas, coming from room-temperature bottles, into the 280 mK BGC cell. For an efficient cooling process, the oxygen molecules should enter the cell with a temperature of 60 K, which ensures an appreciable vapor density ($8 \times 10^{17}\ \mathrm{cm}^{-3}$). The same type of consideration applies to the helium-3 buffer gas; here, as already mentioned, an inlet temperature of 280 mK gives rise to a vapor pressure of $3 \times 10^{16}\ \mathrm{cm}^{-3}$. These injection temperatures can be obtained by choosing, for each of the two gas lines, the most appropriate thermal-exchange configuration (both in terms of geometry and materials) through all the stages of the refrigerator as well as on the BGC cell walls. The whole is housed in a cylindrical vacuum chamber equipped with a number of optical windows for laser spectroscopy. As demonstrated in [26], for the case illustrated in figure 2, an effective (2+1)REMPI-detection can be accomplished with laser pulses of fluence $\sim$1mJ/[π (100 μm)^2]; conservatively, this can be assumed as a threshold value, $F_{\mathrm{thr}} \simeq 30\ \mathrm{mJ\ mm}^{-2}$. This can be obtained with a commercial Nd:YAG[$4\omega_0$]-pumped LiCaAlF:Ce^{3+} laser with the following characteristics: repetition rate $RR \simeq 150$ Hz (the condition $RR > v_m/h$ must be satisfied), pulse length $\simeq$10 ns, line width $\simeq$0.05 nm, pulse energy $\simeq$140 mJ [36]. This corresponds to an initial laser fluence of $F_{\mathrm{in}} \simeq 30\ \mathrm{mJ\ mm}^{-2}$. It is worth pointing out that, after $N_{\mathrm{refl}} = 13\ 500$ reflections, the laser fluence drops to the value $F_{\mathrm{fin}} = \mathcal{R}_m^{N_{\mathrm{refl}}} F_{\mathrm{in}} \simeq 0.5 F_{\mathrm{in}}$ that is significantly below F_{thr}. To overcome this drawback,

two identical lasers (instead of one) can be used to draw the whole pattern of multiple reflections. In the above configuration, the number of oxygen molecules that have been exposed during a second to the axion field is given by

$$N_{\mathrm{molec}} = \frac{n_{\max}}{4}\,\pi\,(d/2)^2\,\nu_m, \tag{4}$$

where $\nu_m = \sqrt{(8k_{\mathrm{B}}T)/(\pi m)}$ and $n_{\max} \simeq (1/30)\cdot n_{\mathrm{He}} = 10^{15}\ \mathrm{cm}^{-3}$ is the maximum molecular density that can be effectively cooled down to T_{He}[28]. Therefore, the number of axion-induced absorption events is calculated as

$$N_{\mathrm{event}} = N_{\mathrm{molec}}\,\frac{\bar{h}}{\nu_m}\,\mathcal{R}_{ab}\,\mathcal{F}\Big(n_{\mathrm{days}}\cdot 24\cdot 3600\Big), \tag{5}$$

where $\bar{h} \simeq \sqrt{h\,d + h^2\,\tan\theta}$ represents the average distance travelled by the molecules within the magnetic field region. The expected rate $\mathcal{R}_{ab}$ can be calculated by formula (8) of [1]. In the worst case, namely for $W_{ba}(B_{\min}) = 11\ \mathrm{cm}^{-1}$ ($B_{\min} = 12$ T), the axion mass is 1.4 meV which yields $\mathcal{R}_{ab} = 1\ \mathrm{Hz}/N_{\mathrm{A}}$. Then, for an acquisition time of $n_{\mathrm{days}} = 10$, $N_{\mathrm{event}} \simeq 1$ is found. However, as $W_{ba}(B)$ increases, higher temperatures can be used for the He-3 bath. In particular, for $W_{ba}(B_{\max}) = 15.5\ \mathrm{cm}^{-1}$ ($B_{\max} = 18$ T), the condition $Q(B, T) < 0.1$ is met up to a temperature of 390 mK which corresponds to a He-3 vapour density of $\simeq 3\times 10^{-17}\ \mathrm{cm}^{-3}$; this one-order-of-magnitude enhancement in the $n_{\max}$ value (and hence in N_{molec} by virtue of equation (4)) can be exploited to reduce the acquisition time in equation (5) down to 1 day (for the same number of events).

5. Conclusion

A novel experimental approach has been described to expose DM in the mass range from 1.4 to 1.9 meV through a laser-spectroscopy detection of the absorption events induced by cosmic axions between Zeeman states in a molecular gas system. Although, in principle, the outlined measurement scheme applies to nearly all species, the oxygen molecule seems to magically combine several crucial features: first, its favourable Zeeman energy-level diagram in the $X^3\Sigma_g^-(\upsilon = 0)$ ground state has already been calculated and measured with great accuracy; second, its very low boiling point in conjunction with a large rotational collision cross-section allows the cooling of a mole-sized gas sample down to 280 mK via BGC; last but not least, highly sensitive, rotationally-resolved REMPI spectroscopy has already been carried out starting from the aforementioned axion transition's levels. Due to the expected far low absorption rate, related to the inherent weakness of matter–DM interaction, very stringent requirements must be matched in order to yield a few counts for reasonable acquisition times. Accordingly, the presented setup involves more than one state-of-the-art technology, the main elements being an effective He-3 refrigerator, a high-performance ultraviolet spectrometer, and a cutting-edge superconducting magnet. It is worth stressing that, while constituting a challenging mix of skills, the different components are essentially already available within minor improvements; also, scalable technological advances can make the proposed experiment even more attractive.

Acknowledgments

The authors acknowledge fruitful discussions with P Sikivie, R Barbieri, A Ortolan, C Speake and G Santambrogio.

References

[1] Sikivie P 2014 Axion dark matter detection using atomic transitions *Phys. Rev. Lett.* **113** 201301
[2] Trimble V 1987 Existence and nature of dark matter in the Universe *Annu. Rev. Astron. Astrophys.* **25** 425
[3] Feng J L 2010 Dark matter candidates from particle physics and methods of detection *Annu. Rev. Astron. Astrophys.* **48** 495
[4] Stadnik Y V and Flambaum V V 2014 Axion-induced effects in atoms, molecules, and nuclei: parity nonconservation, anapole moments, electric dipole moments, and spin-gravity and spin-axion momentum couplings *Phys. Rev.* D **89** 043522
[5] Peccei R D and Quinn H R 1977 CP conservation in the presence of pseudoparticles *Phys. Rev. Lett.* **38** 1440
[6] Peccei R D and Quinn H R 1977 Constraints imposed by CP conservation in the presence of pseudoparticles *Phys. Rev.* D **16** 1791
[7] Weinberg S 1978 A new light boson? *Phys. Rev. Lett.* **40** 223
[8] Wilczek F 1978 Problem of strong *P and T invariance in the presence of instantons Phys. Rev. Lett.* **40** 279
[9] Rosenberg L J 2015 Dark-matter qcd-axion searches *Proc. Natl Acad. Sci. USA* **112** 12278
[10] Sikivie P 1983 Experimental tests of the invisible axion *Phys. Rev. Lett.* **51** 1415
[11] Sikivie P 1985 Detection rates for invisible-axion searches *Phys. Rev.* D **32** 2988
[12] Wuensch W U, De Panfilis-Wuensch S, Semertzidis Y K, Rogers J T, Melissinos A C, Halama H J, Moskowitz B E, Prodell A G, Fowler W B and Nezrick F A 1989 Results of a laboratory search for cosmic axions and other weakly coupled light particles *Phys. Rev.* D **40** 3153
[13] Hagmann C, Sikivie P, Sullivan N S and Tanner D B 1990 Results from a search for cosmic axions *Phys. Rev.* D **42** 1297

[14] Asztalos S J *et al* 2001 Large-scale microwave cavity search for dark-matter axions *Phys. Rev.* D **64** 092003
[15] Barbieri R, Cerdonio M, Fiorentini G and Vitale S 1989 Axion to magnon conversion. A scheme for the detection of galactic axions *Phys. Lett.* B **226** 357
[16] Kakhidze A I and Kolokolov I V 1991 Antiferromagnetic axion detector *Zh. Eskp. Teor. Fiz.* **99** 1077
[17] Graham P W and Rajendran S 2013 New observables for direct detection of axion dark matter *Phys. Rev.* D **88** 035023
[18] Budker D, Graham P W, Ledbetter M, Rajendran S and Sushkov A O 2014 Proposal for a cosmic axion spin precession experiment (casper) *Phys. Rev.* X **4** 021030
[19] Graham P W and Rajendran S 2011 Axion dark matter detection with cold molecules *Phys. Rev.* D **84** 055013
[20] Matsuki S and Yamamoto K 1991 Direct detection of galactic axions with rydberg atoms in an inhibited cavity regime *Phys. Lett.* B **263** 523
[21] Krupenie P H 1972 The spectrum of molecular oxygen *J. Phys. Chem. Ref. Data* **1** 423
[22] de Angelis M, Gagliardi G, Gianfrani L and Tino G M 1996 Test of the symmetrization postulate for spin-0 particles *Phys. Rev. Lett.* **76** 2840
[23] Hilborn R C and Yuca C L 1996 Spectroscopic test of the symmetrization postulate for spin-0 nuclei *Phys. Rev. Lett.* **76** 2844
[24] Brecha R J, Pedrotti L M and Krause D 1997 Magnetic rotation spectroscopy of molecular oxygen with a diode laser *J. Opt. Soc. Am.* B **14** 1921
[25] Berden G, Engeln R, Christianen P C M, Maan J C and Meijer G 1998 Cavity-ring-down spectroscopy on the oxygen A band in magnetic fields up to 20 T *Phys. Rev.* A **58** 3114
[26] Wiederkehr A W, Schmutz H, Motsch M and Merkt F 2012 Velocity-tunable slow beams of cold O_2 in a single spin-rovibronic state with full angular-momentum orientation by multistage Zeeman deceleration *Mol. Phys.* **110** 1807
[27] Patterson D and Doyle S M 2007 Bright, guided molecular beam with hydrodynamic enhancement *J. Chem. Phys.* **126** 154307
[28] Hutzler N R, Lu H-I and Doyle J M 2012 The buffer gas beam: an intense, cold, and slow source for atoms and molecules *Chem. Rev.* **112** 4803
[29] Bohn J L 2000 Cold collisions of O_2 with helium *Phys. Rev.* A **62** 032701
[30] Lique F 2010 Temperature dependence of the fine-structure resolved rate coefficients for collisions of O_2 ($X^3\Sigma_g^-$) with He *J. Chem. Phys.* **132** 044311
[31] deCarvalho R, Doyle J M, Friedrich B, Guillet T, Kim J, Patterson D and Weinstein J D 1999 Buffer-gas loaded magnetic traps for atoms and molecules: a primer *Eur. Phys. J.* D **7** 289
[32] Sur A, Ramana C V, Chupka W A and Coulson S D 1986 Rydberg-valence interactions in the Π_g states of O_2 *J. Chem. Phys.* **84** 69
[33] Katsumata S, Sato K, Achiba Y and Kimura K 1986 Excited-state photoelectron spectra of the one-photon forbidden $C^3\Pi_g$ Rydberg state of molecular oxygen *J. Electron Spectrosc. Relat. Phenom.* **41** 325
[34] Korobenko A, Milner A A, Hepburnb J W and Milnera V 2014 Rotational spectroscopy with an optical centrifuge *Phys. Chem. Chem. Phys.* **16** 4071
[35] Johnson C, Newman B, Brahms N, Doyle J M, Kleppner D and Greytak T J 2010 Zeeman relaxation of cold atomic iron and nickel in collisions with ^{3}He *Phys. Rev.* A **81** 062706
[36] Ultraviolet Solutions (http://uvsol.net/)